

Date of publication xxxx 00, 0000, date of current version xxxx 00, 0000.

Digital Object Identifier 10.1109/ACCESS.2017.Doi Number

A Novel Soft Margin Loss Function for Deep Discriminative Embedding Learning

Zhao Yang^{1,2}, Tie Liu^{1,2}, Jiehao Liu^{1,2}, Li Wang^{1,2}, and Sai Zhao^{1,2}

¹School of Electronics and Communication Engineering, Guangzhou University, Guangzhou 510006, China

²Huangpu Research & Graduate School of Guangzhou University, Guangzhou 510006, China

Corresponding author: Zhao Yang (yangdxng100@126.com).

This work was supported in part by the National Natural Science Foundation of China under Grant 61501177 and Grant 61902084, in part by Guangzhou University's training program for excellent new-recruited doctors under Grant YB201712, in part by the Science and Technology Planning Project of Guangzhou Municipal Government under Grant 201904010466, and in part by the Featured Innovation Project of Guangdong Education Department under Grant 2018KTSCX174.

ABSTRACT Deep embedding learning aims to learn discriminative feature representations through a deep convolutional neural network model. Commonly, such a model contains a network architecture and a loss function. The architecture is responsible for hierarchical feature extraction, while the loss function supervises the training procedure with the purpose of maximizing inter-class separability and intra-class compactness. By considering that loss function is crucial for the feature performance, in this paper we propose a new loss function called soft margin loss (SML) based on a classification framework for deep embedding learning. Specifically, we first normalize the learned features and the classification weights to map them into the hypersphere. After that, we construct our loss with the difference between the maximum intra-class distance and minimum inter-class distance. By constraining the distance difference with a soft margin that is inherent in the proposed loss, both the inter-class discrepancy and intra-class compactness of learned features can be effectively improved. Finally, under the joint training with an improved softmax loss, the model can learn features with strong discriminability. Toy experiments on MNIST dataset are conducted to show the effectiveness of the proposed method. Additionally, experiments on re-identification tasks are also provided to demonstrate the superior performance of embedding learning. Specifically, 65.48% / 62.68% mAP on CUHK03 labeled / detected dataset (person re-id) and 74.36% mAP on VeRi-776 dataset (vehicle re-id) are achieved respectively.

INDEX TERMS Soft margin loss, deep embedding learning, feature representation, person re-identification, vehicle re-identification.

I. INTRODUCTION

Deep embedding learning focuses on learning discriminative representations from input data, whose fundamental purpose is to pull similar samples close and push dissimilar samples away. This intuitive but practical principle enables embedding learning to be widely applied in various fields including person re-identification [1], [2], [3], vehicle re-identification [4], [5], face recognition [6], [7], [8], [9], etc. In general, a deep embedding learning framework comprises two basic components: network architecture and loss function. The network architecture usually consists of cascaded deep convolutional neural networks which can extract highly abstract representations of the input images through its strong non-linear transformation ability and map them into an embedding space. Then the loss function is used

to enhance the discriminability capacity of learned features in the embedding space by constraining their intra-class and inter-class relationships. Since existing deep models have enough power to extract informative features of input images, the loss functions play a critical role in discriminative embedding learning.

Most of loss functions used in embedding learning directly constrain the distance between samples [3], [7], [10], [11]. An intuitive and typical loss function is contrastive loss [10] which pulls a pair of samples together if they belong to the same class and pushes them away by a margin if they come from different classes. Another extensively used loss function is triplet loss [3], [7]. It also adopts a margin to decrease the distance between an anchor and a positive sample and increase the distance between the anchor and a negative

sample. As a predefined margin is involved in the expression of loss function, it is tricky to select an optimum margin parameter for both contrastive loss and triplet loss in the training procedure. Recently, loss functions that used for classification tasks are gradually applied to guide embedding learning via the form of classification. The most representative loss functions are the several variants of softmax, such as L-Softmax [12], A-Softmax [9], ArcFace [6], and so on. They have been proved to be practical and effective for embedding learning. However, the softmax based loss functions only try to separate the features of different classes from the training set instead of learning discriminative features directly. Thus large intra-class variations cannot be handled well in the training process.

Therefore, to alleviate these problems in the discriminative embedding learning, we present a novel loss function named soft margin loss (SML) in this paper. We first normalize the learned features and classification weights thus these vectors are mapped into the hypersphere. By regarding the classification weights as class centers, the intra-class distance can be calculated as the distance between the center and the feature, and the inter-class distance can be calculated as the distance between different class centers. A simple diagrammatic illustration is shown in the left of Figure 1, where the solid dots denote the normalized features and the hollow dots denote the normalized classification weights (a.k.a., the class centers). Different classes are represented with different colors. Theoretically, the learned features are well separable once the maximal intra-class distance is smaller than the minimal inter-class distance, and the discriminability power of learned features will be enhanced as the difference of these two distances decreases. Therefore, we select the difference of the maximal intra-class distance and the minimal inter-class distance as a constraint objective in our loss. Then we constrain the distance difference with a soft margin in our proposed loss whose general formulation and the curve characteristic are shown in the right of Figure 1.

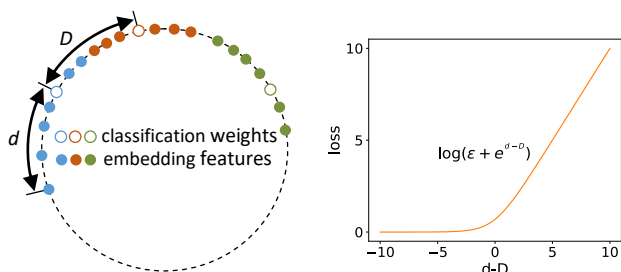


FIGURE 1. The illustration of our proposed soft margin loss. Left: A diagrammatic demonstration of the maximal intra-class distance (d) and the corresponding minimal inter-class distance (D) in a 2-D embedding space. Right: the general formulation and variation curve of the proposed soft margin loss. Best viewed in color.

From the loss curve, we can find that the proposed soft margin loss has some superiorities for embedding learning. On the one hand, the proposed loss strictly penalizes the

embedding distances when the difference of the maximal intra-class distance and the minimal inter-class distance is larger than zero. On the other hand, our loss still provides the constraint power with a soft margin when the difference is smaller than zero. Compared with some fixed margin-based losses, our proposed loss is more flexible in feature learning and its parameter setting of the model training is less empirical. Under the constraint of the soft margin loss, the within-class compactness and between-class discrepancy of learned features are effectively improved, which is favorable to discriminative embedding learning.

We organize the rest paper as follows: Section II gives an introduction of some related works about loss function in the field of deep embedding learning. Section III describes the proposed soft margin loss in detail and introduces the joint training scheme with the improved softmax. Section IV demonstrates the effectiveness and superiority of the soft margin loss via MNIST experiments and some re-identification experiments. After that, Section V compares our loss with some similar works. Finally, Section VI draws some conclusions about our works.

II. RELATED WORKS

In recent years, embedding learning has attracted a great interest in the computer vision community and has been extensively applied in many popular fields including person re-identification, vehicle re-identification, image retrieval and face recognition, etc. The key idea of embedding learning is to learn a satisfactory embedding space where the intra-class compactness and inter-class separability are as large as possible. In the discriminative embedding learning, many works [3], [7], [9], [10], [12], [13], [14] focus on the design of loss function which can provide a powerful and clear supervision for discriminative feature learning. In this section, we will give a view of some loss functions that are frequently used for embedding learning.

Metric loss: In deep learning framework, the metric loss is usually used to constrain the distances between learned features. It accords with the aim of embedding learning which keeps semantically related images close and unrelated images far away in the embedding space. Therefore, various metric losses [1], [3], [7], [10], [11], [15] are extensively applied in embedding learning.

One of the most concise and intuitive metric losses is the contrastive loss [10]. It takes a couple of images as the inputs and pulls the distance between the images if they belong to the identical class or pushes them away by a margin if they come from different classes. For example, Varior *et al.* [11] applied the contrastive loss in a gated siamese convolutional neural network for person re-id task. Similarly, Taigman *et al.* [16] used the contrastive loss in the face verification with a siamese network. Although the contrastive loss is verified to be effective in many tasks, the number of pairwise comparison will be tremendous as the scale of dataset grows up, which makes the model training inefficient. Besides, the

margin parameters need to be tuned and chosen experimentally for different tasks.

Another widely used metric is the triplet loss [3], which takes a triplet as the input that comprises an anchor image, positive image and negative image. Instead of directly constraining the distance between two images, the triplet loss constrains the distance between a positive pair to be smaller than the distance between a negative pair by a predefined margin. In this way, the triplet loss can handle triplet images in each iteration and the introduced margin can impose relatively slack but flexible restrictions among the triplet samples. The triplet loss is extensively used for embedding learning due to its inherent merits. For example, Schroff *et al.* [7] and Cheng *et al.* [15] used the triplet loss to learn a discriminative embedding for face recognition and person re-identification respectively. Hermans *et al.* [3] adopted a hard sampling mining technique in the triplet loss and verified its effectiveness for person re-identification tasks. Motivated by the triplet loss, Chen *et al.* [1] put forward a novel quadruplet loss in which an anchor image, a positive image and two negative images are used to compute the loss. It considers not only a relative distance but also an absolute distance between the positive pair and negative pair. The quadruplet loss can improve the performance by learning features with a larger between-class discrepancy and a smaller within-class variation, which is beneficial to discriminative embedding learning.

Classification loss: Although it is widely used in classification tasks, the classification loss (e.g., softmax loss or its variants) has been demonstrated to be effective for embedding learning. Therefore, various works tried to improve the original softmax loss for discriminative embedding learning. For example, Liu *et al.* [12] proposed L-Softmax to improve the discriminability of learned features by adding an angle margin in the original softmax loss. Based on L-Softmax, Liu *et al.* [9] proposed A-Softmax for discriminative embedding learning by normalizing the weights and imposing an angular margin. To further efficiently enlarge the inter-class distance and decrease the intra-class distance, Wang *et al.* [8] and Deng *et al.* [6] both normalized the features and classification weights, then proposed LMCL (large margin cosine loss) and ArcFace (additive angular margin loss) respectively to learn more discriminative embeddings for face recognition.

Combination of various losses: By considering the great successes of the metric loss and classification loss in embedding learning, many research works [13], [14], [17], [18] tried to combine these various losses for discriminative embedding learning. For instance, Choi *et al.* [17] proposed a joint training scheme of an angular margin contrastive loss and softmax loss to obtain discriminative deep features for image classification. Luo *et al.* [18] introduced a framework for person re-identification where the triplet loss and softmax loss are used together to improve the discriminability of learned features. Wen *et al.* [14] learned discriminative face

representations with the joint optimization of a center loss and softmax loss in which the center loss is applied to further shrink the intra-class variation of each class. By considering the within-class variation and between-class relationship simultaneously, He *et al.* [13] put forward a triplet-center loss which combines the center loss with triplet loss, and used a joint training scheme with softmax loss for 3D object retrieval.

III. PROPOSED METHODS

In this section, we firstly review the original softmax loss function and its improved version which is beneficial to discriminative feature learning. After that, we detail our proposed soft margin loss. Finally, we present the joint training scheme of the improved softmax loss and the soft margin loss in our method.

A. PRELIMINARIES

A typical softmax loss comprises a softmax activation and cross-entropy loss. Softmax loss converts the model output into the class predictions by the softmax activation and calculates the loss via the cross-entropy. The original softmax loss can be expressed as:

$$L_S = -\frac{1}{n} \sum_{i=1}^n \log \frac{e^{W_{y_i}^T f_i + b_{y_i}}}{\sum_{j=1}^C e^{W_j^T f_i + b_j}}, \quad (1)$$

where i is the index of a sample in a batch of training data, and f_i indicates the deep feature of i -th sample whose class label is y_i . W_j and b_j represent the j -th weight column vector in the last fully connected (FC) layer and corresponding bias respectively. C is the class number, and n is the size of the batch.

Some works [6], [8] have shown that better model performance can be obtained by eliminating the bias item and the magnitude influences of both the features and classification weights. Specifically, the logit [19] item $W_j^T f_i + b_j$ is transformed as $\|W_j\| \|f_i\| \cos(\theta_j)$ with ignoring the bias b_j . θ_j is the angle between W_j and f_i . By fixing the weight $\|W_j\| = 1$ and the embedding feature $\|f_i\| = s$ with L2 normalizations respectively, the logit item can be simplified as $s \cdot \cos(\theta_j)$, where s serves as a scale factor that controls the range of the feature space. Finally, the improved softmax can be expressed as follows:

$$\begin{aligned} L_{NSL} &= -\frac{1}{n} \sum_{i=1}^n \log \frac{e^{\|W_{y_i}\| \|f_i\| \cos(\theta_{y_i})}}{\sum_{j=1}^C e^{\|W_j\| \|f_i\| \cos(\theta_j)}} \\ &= -\frac{1}{n} \sum_{i=1}^n \log \frac{e^{s \cdot \cos(\theta_{y_i})}}{\sum_{j=1}^C e^{s \cdot \cos(\theta_j)}} \end{aligned} \quad (2)$$

With the normalizations of classification weights and features, the classification scores only depend on the angle between the feature and corresponding classification weight. Thus the learned features are angularly separable in the hypersphere. In this paper, we name the improved softmax

expressed in equation (2) as normalized softmax loss (NSL) to distinguish the original softmax loss.

B. THE PROPOSED SOFT MARGIN LOSS

Softmax loss can learn a fine embedding space for input images. However, once the images are well classified in the embedding space, softmax loss lacks a distinct and strong supervision to continuously pull the similar images close and push the dissimilar images away. So it is hard for the model to mine enough discriminative information of input images. Therefore, we propose the soft margin loss for discriminative embedding learning. Concretely, we first normalize the features and classification weights as the same processing in the NSL. After that, we regard the normalized classification weights in the last FC layer as the center of each class. In this way, the intra-class distance could be represented as the cosine distance between the center and the feature coming from the same class, and the inter-class distance can be represented as the cosine distance between the different centers. To constrain the intra-class and inter-class distance strictly, we use the difference of the maximal intra-class distance and the minimal inter-class distance as the constraint objective of the proposed loss. Finally, the specific formulation of the soft margin loss is given by:

$$L_{SML} = \frac{1}{C} \sum_{j=1}^C \log \left(\varepsilon + e^{\frac{\max_{i=j} (f_i, W_j) - \min_{k \neq j} (W_k, W_j)}{C}} \right), \quad (3)$$

where ε is a moderating factor to adjust the strength of the soft margin.

Our proposed soft margin loss has three superior properties. First, since the features and classification weights are normalized into the hypersphere, the intra-class and inter-class distances are irrelevant to the magnitudes of both features and classification weights. Thus the soft margin loss calculated by these distances can efficiently guide the embedding learning. Second, the soft margin loss can generate a strict penalty when the difference of the maximal intra-class distance and the minimal inter-class distance is larger than zero. It means that the soft margin loss can help the model learn a correct classification quickly at the initial training stage. Third, even if the distance difference is smaller than zero, the proposed loss still provides a soft margin to help the model mine the discriminative information from the input data. On the one hand, this soft margin can help discriminative embedding learning via further improving the within-class compactness and between-class discrepancy. On the other hand, the softness of the margin can provide flexibility during the model training procedure compared with a fixed margin. Therefore, the proposed soft margin loss could be used for discriminative embedding learning.

C. JOINT TRAINING

The classification loss can learn a fine embedding space but lacks a distinct and strong supervision signal to continuously

enlarge between-class discrepancy and shrink within-class compactness. The metric loss can be used for discriminative embedding learning but encounters the low convergence problem. Therefore, in this paper, we introduce a joint training scheme to combine the normalized softmax loss and the proposed soft margin loss. Thus the final loss representation is:

$$L = L_{NSL} + \lambda L_{SML}, \quad (4)$$

where λ is a parameter to balance the normalized softmax loss and the soft margin loss. Different from most joint training schemes that directly use softmax loss, our method applies the normalized softmax loss in the joint training. Since the features and classification weights are regulated by the L2 normalization, the normalized softmax loss is only relevant to the angles between the features and classification weights. Therefore, the optimization targets of these two losses are consistent during the training procedure.

IV. EXPERIMENTS

In this section, we first carry out some toy experiments based on MNIST dataset to intuitively show the superiority of the proposed loss by comparing with the original softmax loss and the normalized softmax loss. Subsequently, we further demonstrate the effectiveness of our method on re-identification tasks, including person re-identification and vehicle re-identification. Both of them can be regarded as an image retrieval problem [20], which retrieves similar images to a query image among a large dataset.

A. TOY EXAMPLES ON MNIST

MNIST dataset [21] is the most popular hand-written digit benchmark dataset. It includes a total of 70000 images of 10 types of numbers from 0 to 9, where 60000 images are used for training and the rest 10000 images are used for testing.

For convenience, we use a concise CNN model to conduct the MNIST experiments with the original softmax, the normalized softmax and the normalized softmax with soft margin loss respectively. All model parameter settings are the same except the loss function used in the network. To intuitively demonstrate the effects of three different losses, we visualize the learned features by setting their dimension as 2 and projecting them into 2-D embedding space. The results are illustrated in Figure 2. The first row denotes the features without normalization and the second row represents the corresponding features with normalization.

From the feature distributions in Figure 2, we can see that the features learned by the original softmax are well separable in the embedding space while they have poor intra-class compactness. For the features learned by the normalized softmax, we can find that the intra-class compactness has been improved greatly since the features and classification weights are normalized into hypersphere. In spite of the satisfactory feature embedding characteristics, preferable intra-class compactness can be obtained by adding

the soft margin loss to the normalized softmax. From the results trained by the normalized softmax with soft margin loss, we can obviously observe that the intra-class variance

becomes smaller than that of the normalized softmax, which means that the feature discriminations are further strengthened.

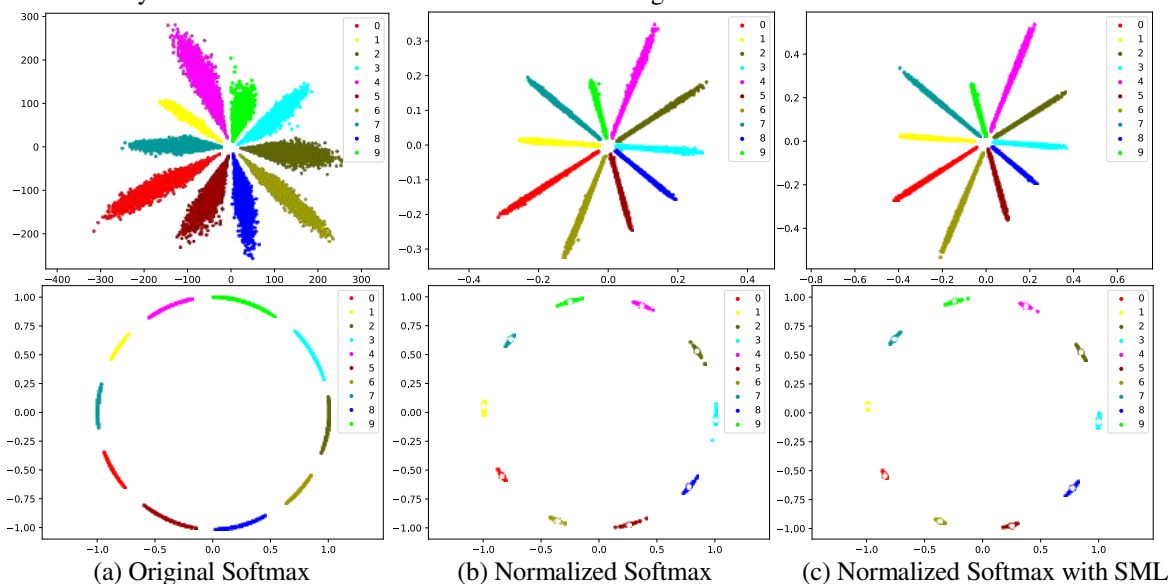


FIGURE 2. Experimental results based on MNIST dataset with original softmax, normalized softmax and normalized softmax with soft margin loss (SML) respectively. The first row represents the data distributions of original features in 2-D embedding space and the second row represents the corresponding normalized features. From the results, we can see that the features learned by original softmax have less within-class compactness while the normalized softmax can effectively improve the within-class compactness by normalizing the features and classification weights. On the basis of the normalized softmax, the soft margin loss constrains both the within-class compactness and between-class discrepancy of features simultaneously thus the learned features are more discriminative. Best viewed in color.

From our observations in the MNIST experiments, some conclusions can be drawn. First of all, it is practicable to use the classification loss for the embedding learning. However, the features learned by softmax loss are less discriminative because the original softmax mainly focuses on the separability of learned features. Second, the normalized softmax improves the discriminability of feature embedding by regulating the magnitudes of both features and classification weights as constants. In this way, the model only focuses on the cosine distances between features during the training procedure. Thus the learned features are more discriminative than that learned from the original softmax. Third, on the basis of the normalized softmax, the proposed soft margin loss explicitly constrains the inter-class and intra-class distances between features. Therefore, with the joint training of the normalized softmax loss and the proposed soft margin loss, the learned features can obtain powerful discriminability. Based on the experimental results on MNIST as well as above analysis, the proposed soft margin loss shows its superiority and latent capacity for discriminative embedding learning.

B. EXPERIMENTS ON RE-IDENTIFICATION TASKS

1) DATASET DESCRIPTIONS

CUHK03 [22] is an extensively used person re-id dataset which is collected by 5 pairs of cameras in CUHK campus. CUHK03 contains 14096 images of 1467 person identities. For practical applications, CUHK03 dataset provides not

only manually cropped pedestrian images, but also automatically detected bounding boxes. However, the dataset is originally designed for a single-shot situation which cannot comprehensively evaluate the performance of person re-id tasks. Therefore Zhong *et al.* [23] introduced a new protocol for training/testing. Specifically, 767 person identities are allocated to the training set and the rest 700 person identities are used as the testing set. We use the new protocol of CUHK03 in our experiments. During the training procedure, we rescale the input images to 288×144 and randomly crop them to 256×128. Then the images are horizontally flipped with the probability 0.5. As most re-id tasks do, we normalize the image RGB channels by subtracting (0.485, 0.456, 0.406) and dividing (0.229, 0.224, 0.225), respectively. Moreover, a random erasing operation [24] is used on the training images as a kind of data augmentation trick to enhance the robustness of the model. In the testing phase, the images are resized to 288×144. The same normalization operation is done before the images are fed into the testing network. It is worth noting that the final feature embedding is the average of features from the original image and its horizontally flipped version.

VeRi-776 [25] is a large scale publicly available vehicle dataset built from the VeRi dataset [26], which is collected in a real-world traffic scene by 2 to 18 cameras at different viewpoints, illuminations, resolutions and occlusion conditions. After the expansion from the VeRi dataset, VeRi-776 contains 776 different vehicles, including 37781 pictures

of 576 vehicles in the training set and 11579 pictures of 200 vehicles in the testing set. Different from the preprocessing of the person re-identification task, the training vehicle images are rescaled to 288×288 and cropped to 256×256 randomly. Then the same horizontal flipping operation, normalization and random erasing trick are conducted sequentially. For testing, the vehicle images are resized to 256×256 . Similarly, the features that learned from the original image and the horizontally flipping image are averaged as the final embedding.

2) NETWORK ARCHITECTURE

We construct our model based on ResNet-50 [27] which is pretrained on ImageNet [28]. Concretely, we modify the structure of ResNet-50 to make it meet the requirements of our method. For example, the last FC layer of ResNet-50 is

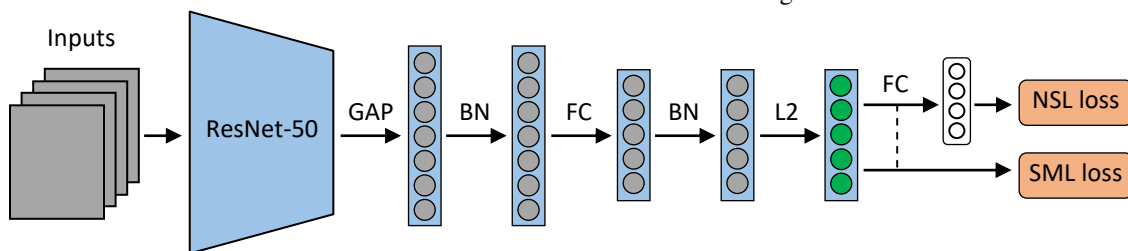


FIGURE 3. The network architecture for our re-id experiments, where the backbone is constructed with ResNet-50. Then some auxiliary layers including GAP layer, BN layer, FC layer and L2 layer are added behind the ResNet-50. In the training stage, the model is trained by the normalized softmax loss (NSL loss) and the soft margin loss (SML loss). In the testing stage, the last fully connected layer is removed so the network becomes a feature extractor which can automatically extract features from input images.

3) EXPERIMENTAL SETTINGS

All experiments are conducted in the Pytorch [29] framework with an NVIDIA GTX 1080 Ti GPU. Except for the tiny difference in the data preprocessing, we keep all the network parameters same in the person and vehicle re-identification tasks, which can illustrate the generalization ability of our proposed method.

In many re-identification datasets, the available images of each class are usually quite different in the number. Therefore, the model may tend to overfit the class with abundant images and ignore the class with few images. Therefore, we use a balanced sampling scheme [2] in which the sampled classes and corresponding images are stationary in each mini batch. Specifically, P classes are randomly selected without replacement in each epoch. Then for every class, we randomly select K images for training. The images will be replaced if the number of images is less than K . So, there are always $P \cdot K$ images in a mini batch, and we set P and K as 16 and 4 respectively in the experiments.

Besides, we adopt Adam [30] optimizer to update model parameters during the training. We set the total epoch as 150 and use a warm-up strategy [2] during the initial 20 epochs. It means that the learning rate will increase continuously from a small value. Concretely, the learning rate linearly increases from 10^{-5} to 10^{-3} in the first 20 epochs. Since the model may tackle different tasks (e.g., person or vehicle re-identification

tasks), a relatively small learning rate is beneficial for the model to obtain a well initial state in different tasks. After the warm-up stage, the learning rate remains at 10^{-3} until 90th. Then the learning rate is decayed by 0.1 at 90th and 130th separately to fine-tune the parameters.

Moreover, we apply a hard mining strategy in our method which can enhance the generalization ability of the learned model. More specifically, we sort a batch of samples according to the predictions of the normalized softmax in descending order, and take the first 80% of the samples to update the parameters of our model. Besides, the scale parameter s in normalized softmax is 14, the moderating factor ε in the proposed soft margin loss is 0.2 and the balance weight λ for soft margin loss is set as 1.0.

tasks), a relatively small learning rate is beneficial for the model to obtain a well initial state in different tasks. After the warm-up stage, the learning rate remains at 10^{-3} until 90th. Then the learning rate is decayed by 0.1 at 90th and 130th separately to fine-tune the parameters.

Moreover, we apply a hard mining strategy in our method which can enhance the generalization ability of the learned model. More specifically, we sort a batch of samples according to the predictions of the normalized softmax in descending order, and take the first 80% of the samples to update the parameters of our model. Besides, the scale parameter s in normalized softmax is 14, the moderating factor ε in the proposed soft margin loss is 0.2 and the balance weight λ for soft margin loss is set as 1.0.

4) EXPERIMENTAL RESULTS

In re-identification tasks, cumulative match characteristic (CMC) and mean average precision (mAP) are two widely used evaluation metrics. CMC gives the average probability that the image which matches with a specific query image arises in the first- k candidates of the gallery set. However, when there are multiple matching images in gallery (e.g., person re-identification task), CMC metric will be deficient and cannot evaluate the method comprehensively. Therefore, many re-id tasks use mAP evaluation which considers all true matches and returns the mean average precision. In our

experiment, we report values of CMC at Rank-1 and mAP for the person and vehicle re-identification tasks.

The experimental results and comparisons with corresponding state-of-the-art works on person and vehicle re-identification tasks are given in Table 1 and Table 2 respectively. In both re-id tasks, the models trained by the normalized softmax are treated as the baseline model.

TABLE 1. The results of our method and some state-of-the-art works on CUHK03 dataset.

Methods	Labeled		Detected	
	mAP	Rank-1	mAP	Rank-1
DaF [31]	31.5	27.5	30.0	26.4
PAN [32]	35.0	36.9	34.0	36.3
SVDNet [33]	37.83	40.93	37.3	41.5
DPFL [34]	40.5	43.0	37.0	40.7
HA-CNN [35]	41.0	44.4	38.6	41.7
MGCAM-Siamese [36]	50.21	50.14	46.87	46.71
MLFN [37]	49.2	54.7	47.8	52.8
PCB+RPP [38]	-	-	56.7	62.8
Baseline	63.34	64.43	60.36	61.43
Ours	65.48	67.86	62.68	64.21

In the results of person re-identification task, we can find that the proposed method outperforms the baseline in CUHK03 labeled version and detected version. For example, in the labeled version, our proposed method has improved performance by +2.14% and +3.43% on mAP and Rank-1. In detected version, our method brings +2.32% and +2.78% improvements on mAP and Rank-1. Besides, we also make a

TABLE 3. Comparisons between our method and two fix margin based methods on CUHK03 and VeRi-776 datasets.

Methods	m	CUHK03 labeled		CUHK03 detected		VeRi-776	
		mAP	Rank-1	mAP	Rank-1	mAP	Rank-1
NSL+Triplet	0.01	63.29	64.86	60.91	61.79	73.63	94.76
	0.1	63.32	65.29	59.81	62.07	73.31	94.58
	0.3	63.53	65.57	60.29	60.86	73.41	94.40
	0.5	63.74	65.43	61.67	62.93	73.74	93.98
	1.0	65.76	67.71	62.77	64.14	74.43	94.28
	1.5	65.76	67.71	62.77	64.14	74.43	94.28
LMCL	0.01	63.12	63.71	61.42	63.36	73.04	94.40
	0.1	63.55	66.50	62.54	63.64	74.92	95.11
	0.3	63.32	64.64	60.71	62.00	75.32	94.87
	0.5	62.15	64.21	58.49	60.43	75.13	94.93
	1.0	61.86	63.50	58.46	59.79	74.54	95.17
	1.5	61.92	63.36	60.22	62.21	74.62	94.76
Ours	-	65.48	67.86	62.68	64.21	74.36	94.99

5) COMPARISONS WITH FIXED MARGIN

In the proposed loss, we use the “soft” margin to guide the training procedure. Here, we try to compare our method with fixed margin based loss functions. We choose the triplet loss and LMCL [8] for comparative experiments, since the two

comparison between the proposed method and some state-of-the-art works such as SVDNet [33] and PCB+RPP [38], etc. Compared with PCB+RPP, our results increase by +5.98% on PCB+RPP mAP (56.7%) in detected version.

TABLE 2. The results of our method and some state-of-the-art works on VeRi-776 dataset.

Methods	VeRi-776	
	mAP	Rank-1
XVGAN [39]	24.65	60.20
VAMI [40]	50.13	77.03
PROVID [41]	53.42	81.56
SDC-CNN [42]	53.45	83.49
JFSDL [5]	53.53	82.90
Hard-View-EALN [4]	57.44	84.39
RAM [43]	61.5	88.6
QD-DLF [44]	61.83	88.50
Baseline	73.00	94.87
Ours	74.36	94.99

For the vehicle re-id task, we compare the current state-of-the-art methods with our proposed approach, and the total results are recorded in Table 2. Obviously, compared to the baseline, the proposed soft margin loss brings improvements on both mAP and Rank-1. In specific, there are +1.36% and +0.12% increase on mAP and Rank-1 respectively. Besides, our method surpasses the most competitive method QD-DLF by +12.53% and +6.49% on mAP and Rank-1. The results show that the proposed soft margin loss is also effective in the vehicle re-identification.

losses are both margin based methods and they represent the typical metric loss and classification loss in recent researches.

For the triplet loss, its formulation is given by:

$$L_{TRI} = \frac{1}{C} \sum_{j=1}^C \max \left[0, \max_{y_i=j} (f_i, W_j) - \min_{k \neq j} (W_k, W_j) + m \right]. \quad (5)$$

The definition of intra-class and inter-class distances is same with that in the soft margin loss. For fair comparison, we jointly optimize the normalized softmax and the triplet loss for model training. The total loss can be expressed as $L = L_{NSL} + \lambda L_{TRI}$, Where λ is the weight parameter and is set as 1 for simplicity. For LMCL with margin m , it can be represented as:

$$L_{LMCL} = -\frac{1}{n} \sum_{i=1}^n \log \frac{e^{s \cdot (\cos \theta_{y_i} - m)}}{e^{s \cdot (\cos \theta_{y_i} - m)} + \sum_{j \neq y_i}^C e^{s \cdot \cos(\theta_j)}}. \quad (6)$$

We keep all the previous experimental settings unchanged and substitute the soft margin loss with the triplet loss and LMCL. The comparative results with different margins are recorded in Table 3. From the results, we can see that the mAP values of “NSL+Triplet” on CUHK03 and VeRi-776 datasets change a lot along with margin m . Besides it exhibits a saturation pheromone when m exceeds a large value, e.g. $m > 1.0$. LCML has not obvious improvements on CHHK03 while obtains better accuracy on VeRi-776 with different margins. By comparison, our proposed soft margin loss can achieve preferable results without a margin parameter, which is close to the best performance from the margin based methods.

6) PARAMETER ANALYSIS

The parameter λ denotes the weight of the soft margin loss in the joint training scheme. To observe how λ impacts the model performance, we keep ε as 0.2 and vary λ from {0.1, 0.2, 0.5, 1.0, 1.5, 2.0, 5.0} for both CUHK03 and VeRi-776. The corresponding results are plotted in Figure 4. For CUHK03 labeled version, the value of mAP fluctuates with the increasing of λ , and mAP achieves the largest value when λ is 1.0. While for detected version, the mAP keeps a steady and slight increase. In the results of VeRi-776 dataset, we can see that the mAP increases gradually as λ increases from 0.1 to 2.0 and declines when λ larger than 2.0.

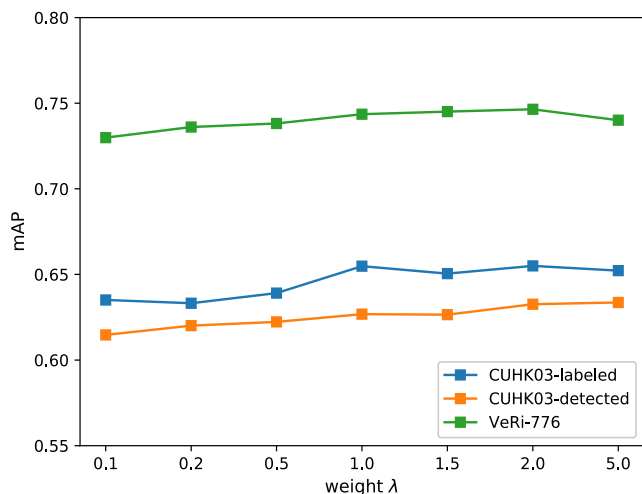


FIGURE 4. The mAP results corresponding to different values of λ on both CUHK03 and VeRi-776 datasets. For CUHK03 dataset, the mAP value has fluctuation but steady raising with the increase of λ . For

VeRi-776 dataset, the value of mAP raises slightly along with the increase of λ .

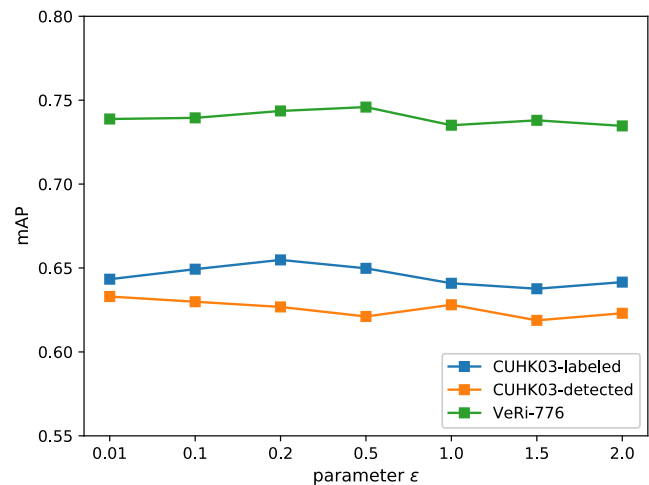


FIGURE 5. The mAP results corresponding to different values of ε on CUHK03 dataset and VeRi-776 dataset respectively. For CUHK03 dataset, the value of mAP has descending trends on the whole when ε is larger than 0.2. For VeRi-776 dataset, the value of mAP changes within a narrow range.

We check the influences of the parameter ε on the model performance with a similar manner. We set λ as 1.0 and vary ε from {0.01, 0.1, 0.2, 1.0, 1.5, 2.0} respectively. The corresponding mAP curves are shown in Figure 5. For CUHK03 labeled version, the best result is obtained when ε is 0.2. While in CUHK03 detected version, the mAP curve roughly shows a decline tendency except a surge where ε is 1.0. For VeRi-776, the mAP raises when ε increases from 0.01 to 0.05 but has an obvious decrease when ε is larger than 0.5.

V. DISCUSSION

Here, we first discuss the relations between our proposed method with two similar loss functions, including ArcFace [6] and triplet-center loss [13]. ArcFace maps the features and classification weights into the hypersphere with the normalization operation. Then it constrains the angles between features and their corresponding weight by adding a fixed margin for discriminative embedding learning. The triplet-center loss combines the triplet loss and center loss to maximize the intra-class compactness and inter-class separability simultaneously, and it performs discriminative embedding learning with a joint training scheme of softmax loss.

Compared to the abovementioned approaches, our proposed method has three following advantages. First, since the difference of maximal intra-class distance and the minimal inter-class distance is taken as one of the optimization objectives, the proposed soft margin loss can learn discriminative features without an empirically fixed margin. It is convenient and practicable for the soft margin loss to generalize itself in various applications. Second, in the soft margin loss, we treat the classification weights as the

feature centers when we calculate the inter-class distance and intra-class distance. This operation is reasonable in the methodology and costless in the calculation. Third, since the features and classification weights are normalized in the hypersphere, the soft margin loss and the normalized softmax have identical optimization goals in the embedding space, i.e., the angle between learned features and weights. Therefore the joint training with these two losses can effectively alleviate the problem of low convergence and benefit discriminative embedding learning.

In this work, we design our loss function with the difference between the maximum intra-class distance and minimum inter-class distance for embedding learning. I think the discriminative power would be further enhanced if we consider an additional constraint on the intra-class compactness alone. So in the future research, we plan to explore new types of loss functions to improve the performance of deep embedding learning, and validate the methods on other related vision tasks, such as face recognition [8], texture classification [45], and so on.

VI. CONCLUSIONS

In this work, we propose a new loss function called soft margin loss for discriminative embedding learning. Specially, we first normalize the learned features and classification weights to map them into the hypersphere. With the normalization operation, the model prediction scores only depend on the angle between the feature and the weight, which is beneficial to the model convergence. Then the proposed soft margin loss is used to increase the between-class discrepancy and shrink the within-class compactness by constraining the difference of the maximal intra-class distance and the minimal inter-class distance. Finally, the soft margin loss and the normalized softmax are joined together to supervise the model for achieving discriminative and robust feature embedding. The proposed method can efficiently optimize the intra-class and inter-class distances of learned features with a soft margin and help for discriminative embedding learning. Extensive experiments on toy examples and re-identification tasks (e.g., person and vehicle re-identification) are conducted to illustrate the effectiveness of our method.

REFERENCES

- [1] W. Chen, X. Chen, J. Zhang, and K. Huang, "Beyond triplet loss: A deep quadruplet network for person re-identification," in *Proc. IEEE Conf. Comput. Vis. Pattern Recognit. (CVPR)*, Honolulu, HI, USA, July, 2017, pp. 21-26.
- [2] X. Fan, W. Jiang, H. Luo, and M. Fei, "SphereReID: Deep hypersphere manifold embedding for person re-identification," *J. Vis. Commun. Image Represent.*, vol. 60, pp. 51-58, Apr. 2019.
- [3] A. Hermans, L. Beyer, and B. Leibe, "In defense of the triplet loss for person re-identification," 2017, *arXiv:1703.07737*. [Online]. Available: <https://arxiv.org/abs/1703.07737>
- [4] Y. Lou, Y. Bai, J. Liu, S. Wang, and L. Duan, "Embedding adversarial learning for vehicle re-identification," *IEEE Trans. Image Process.*, vol. 28, no. 8, pp. 3794-3807, Aug. 2019.
- [5] J. Zhu, H. Zeng, Y. Du, Z. Lei, L. Zheng, and C. Cai, "Joint feature and similarity deep learning for vehicle re-identification," *IEEE Access*, vol.6, pp. 43724-43731, Aug. 2018.
- [6] J. Deng, J. Guo, N. Xue, and S. Zafeiriou, "ArcFace: Additive angular margin loss for deep face recognition," in *Proc. IEEE Conf. Comput. Vis. Pattern Recognit. (CVPR)*, Long Beach, CA, USA, June 2019, pp. 15-20.
- [7] F. Schroff, D. Kalenichenko, and J. Philbin, "FaceNet: A unified embedding for face recognition and clustering," in *Proc. IEEE Conf. Comput. Vis. Pattern Recognit. (CVPR)*, Boston, MA, USA, June 2015, pp. 7-12.
- [8] H. Wang, Y. Wang, Z. Zhou, X. Ji, D. Gong, J. Zhou, Z. Li, and W. Liu, "CosFace: Large margin cosine loss for deep face recognition," in *Proc. IEEE Conf. Comput. Vis. Pattern Recognit. (CVPR)*, Salt Lake City, UT, USA, June 2018, pp. 18-23.
- [9] W. Liu, Y. Wen, Z. Yu, M. Li, B. Raj, and L. Song, "SphereFace: Deep hypersphere embedding for face recognition," in *Proc. IEEE Conf. Comput. Vis. Pattern Recognit. (CVPR)*, Honolulu, HI, USA, July 2017, pp. 21-26.
- [10] R. Hadsell, S. Chopra, and Y. LeCun, "Dimensionality reduction by learning an invariant mapping," in *Proc. IEEE Conf. Comput. Vis. Pattern Recognit. (CVPR)*, New York, NY, USA, June 2006, pp. 17-22.
- [11] R. Varior, M. Haloi, and G. Wang, "Gated siamese convolutional neural network architecture for human re-identification," in *Proc. Eur. Conf. Comput. Vis. (ECCV)*, Amsterdam, The Netherlands, Oct. 2016, pp. 11-14.
- [12] W. Liu, Y. Wen, Z. Yu, and M. Yang, "Large-margin softmax loss for convolutional neural networks," in *Proc. Conf. Mach. Learn. (ICML)*, New York, NY, USA, June 2016, pp. 19-24.
- [13] X. He, Y. Zhou, Z. Zhou, S. Bai, and X. Bai, "Triplet-center loss for multi-view 3D object retrieval," in *Proc. IEEE Conf. Comput. Vis. Pattern Recognit. (CVPR)*, Salt Lake City, UT, USA, June 2018, pp. 18-23.
- [14] Y. Wen, K. Zhang, Z. Li, and Y. Qiao, "A discriminative feature learning approach for deep face recognition," in *Proc. Eur. Conf. Comput. Vis. (ECCV)*, Amsterdam, The Netherlands, Oct. 2016, pp. 11-14.
- [15] D. Cheng, Y. Gong, S. Zhou, J. Wang, and N. Zheng, "Person re-identification by multi-channel parts-based cnn with improved triplet loss function," in *Proc. IEEE Conf. Comput. Vis. Pattern Recognit. (CVPR)*, Las Vegas, NV, USA, June 2016, pp. 27-30.
- [16] Y. Taigman, M. Yang, M. A. Ranzato, and L. Wolf, "DeepFace: Closing the gap to human-level performance in face verification," in *Proc. IEEE Conf. Comput. Vis. Pattern Recognit. (CVPR)*, Columbus, OH, USA, June 2014, pp. 23-28.
- [17] H. Choi, A. Som, and P. Turaga, "AMC-Loss: Angular margin contrastive loss for improved explainability in image classification," in *Proc. IEEE Conf. Comput. Vis. Pattern Recognit. Workshops (CVPRW)*, Seattle, WA, USA, June 2020, pp. 14-19.
- [18] H. Luo, W. Jiang, Y. Gu, F. Liu, X. Liao, S. Lai, and J. Gu, "A strong baseline and batch normalization neck for deep person re-identification," *IEEE Trans. Multimedia*, pp. 1-1, Dec. 2019, DOI: 10.1109/TMM.2019.2958756.
- [19] G. Pereyra, G. Tucker, J. Chorowski, L. Kaiser, and G. Hinton, "Regularizing neural networks by penalizing confident output distributions," 2017, *arXiv:1701.06548*. [Online]. Available: <https://arxiv.org/abs/1701.06548>
- [20] N. Hor, S. Fekri-Ershad, "Image retrieval approach based on local texture information derived from predefined patterns and spatial domain information," *International Journal of Computer Science Engineering*, vol. 8, no. 6, pp. 246-254, Nov.-Dec. 2019.
- [21] Y. Lecun, L. Bottou, Y. Bengio, and P. Haffner, "Gradient-based learning applied to document recognition," *Proc. IEEE*, vol.86, no. 11, pp. 2278-2324, Nov. 1998.
- [22] W. Li, R. Zhao, T. Xiao, and X. Wang, "DeepReID: Deep filter pairing neural network for person re-identification," in *Proc. IEEE Conf. Comput. Vis. Pattern Recognit. (CVPR)*, Columbus, OH, USA, June 2014, pp. 23-28.
- [23] Z. Zhong, L. Zheng, D. Cao, and S. Li, "Re-ranking person re-identification with k-reciprocal encoding," in *Proc. IEEE Conf.*

- Comput. Vis. Pattern Recognit. (CVPR)*, Honolulu, HI, USA, July 2017, pp. 21-26.
- [24] Z. Zhong, L. Zheng, G. Kang, S. Li, and Y. Yang, "Random erasing data augmentation," in *Proc. AAAI Conf. Artif. Intell.*, Hilton New York Midtown, New York, USA, Feb. 2020, pp. 13001-13008.
- [25] X. Liu, W. Liu, T. Mei, and H. Ma, "A deep learning-based approach to progressive vehicle re-identification for urban surveillance," in *Proc. Eur. Conf. Comput. Vis. (ECCV)*, Amsterdam, The Netherlands, Oct. 2016, pp. 11-14.
- [26] X. Liu, W. Liu, H. Ma, and H. Fu, "Large-scale vehicle re-identification in urban surveillance videos," in *Proc. IEEE Int. Conf. Multimedia Expo. (ICME)*, Seattle, WA, USA, July 2016, pp. 11-15.
- [27] H. He, X. Zhang, S. Ren, and J. Sun, "Deep residual learning for image recognition," in *Proc. IEEE Conf. Comput. Vis. Pattern Recognit. (CVPR)*, Las Vegas, NV, USA, June 2016, pp. 27-30.
- [28] J. Deng, W. Dong, R. Socher, L. Li, K. Li, and F. Li, "ImageNet: A large-scale hierarchical image database," in *Proc. IEEE Conf. Comput. Vis. Pattern Recognit. (CVPR)*, Miami, FL, USA, June 2009, pp. 20-25.
- [29] Pytorch. <https://pytorch.org/>.
- [30] D. P. Kingma, and J. Ba, "Adam: A method for stochastic optimization," in *Proc. Int. Conf. Learn. Represent. (ICLR)*, San Diego, CA, USA, May 2015, pp. 7-9.
- [31] R. Yu, Z. Zhou, S. Bai, and X. Bai, "Divide and fuse: A re-ranking approach for person re-identification," in *Proc. Br. Mach. Vis. Conf. (BMVC)*, London, UK, Sept. 2017, pp. 4-7.
- [32] Z. Zheng, L. Zheng, and Y. Yang, "Pedestrian alignment network for large-scale person re-identification," *IEEE Trans. Circuits Syst. Video Technol.*, vol. 29, no. 10, pp. 3037-3045, Oct. 2018.
- [33] Y. Sun, L. Zheng, W. Deng, and S. Wang, "SVDNet for pedestrian retrieval," in *Proc. IEEE Int. Conf. Comput. Vis. (ICCV)*, Venice, Italy, Oct. 2017, pp. 22-29.
- [34] Y. Chen, X. Zhu, and S. Gong, "Person re-identification by deep learning multi-scale representations," in *Proc. IEEE Int. Conf. Comput. Vis. Workshops (ICCVW)*, Venice, Italy, Oct. 2017, pp. 22-29.
- [35] W. Li, X. Zhu, and S. Gong, "Harmonious attention network for person re-identification," in *Proc. IEEE Conf. Comput. Vis. Pattern Recognit. (CVPR)*, Salt Lake City, UT, USA, June 2018, pp. 18-23.
- [36] C. Song, Y. Huang, W. Ouyang, and L. Wang, "Mask-guided contrastive attention model for person re-identification," in *Proc. IEEE Conf. Comput. Vis. Pattern Recognit. (CVPR)*, Salt Lake City, UT, USA, June 2018, pp. 18-23.
- [37] X. Chang, T. M. Hospedales, and T. Xiang, "Multi-level factorization net for person re-identification," in *Proc. IEEE Conf. Comput. Vis. Pattern Recognit. (CVPR)*, Salt Lake City, UT, USA, June 2018, pp. 18-23.
- [38] Y. Sun, L. Zheng, Y. Yang, Q. Tian, and S. Wang, "Beyond part models: Person retrieval with refined part pooling (and a strong convolutional baseline)," in *Proc. Eur. Conf. Comput. Vis. (ECCV)*, Munich, Germany, Sept. 2018, pp. 8-14.
- [39] Y. Zhou, and L. Shao, "Cross-view gan based vehicle generation for re-identification," in *Proc. Br. Mach. Vis. Conf. (BMVC)*, London, UK, Sept. 2017, pp. 4-7.
- [40] Y. Zhou, and L. Shao, "Viewpoint-aware attentive multi-view inference for vehicle re-identification," in *Proc. IEEE Conf. Comput. Vis. Pattern Recognit. (CVPR)*, Salt Lake City, UT, USA, June 2018, pp. 18-23.
- [41] X. Liu, W. Liu, T. Mei, and H. Ma, "PROVID: Progressive and multimodal vehicle reidentification for large-scale urban surveillance," *IEEE Trans. Multimedia*, vol. 20, no. 3, pp. 645-658, Mar. 2018.
- [42] J. Zhu, H. Zeng, Z. Lei, S. Liao, L. Zheng, and C. Cai, "A shortly and densely connected convolutional neural network for vehicle re-identification," in *Proc. Int. Conf. Pattern Recognit. (ICPR)*, Beijing, China, Aug. 2018, pp. 20-24.
- [43] X. Liu, S. Zhang, Q. Huang, and W. Gao, "RAM: A region-aware deep model for vehicle re-identification," in *Proc. IEEE Int. Conf. Multimedia Expo (ICME)*, San Diego, CA, USA, July 2018, pp. 23-27.
- [44] J. Zhu, H. Zeng, J. Huang, S. Liao, Z. Lei, C. Cai, and L. Zheng, "Vehicle re-identification using quadruple directional deep learning

features," *IEEE Trans. Intell. Transp. Syst.*, vol. 21, no. 1, pp. 410-420, Mar. 2019.

- [45] S. Fekri-Ershad, "Bark texture classification using improved local ternary patterns and multilayer neural network," *Expert Syst. Appl.*, vol. 158, 113509, Nov., 2020.



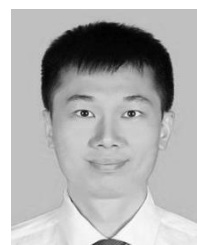
ZHAO YANG received a Ph.D. degree from South China University of Technology in 2014. He is currently a lecturer in the School of Electronics and Communication Engineering, Guangzhou University. His research interests include machine learning, pattern recognition.



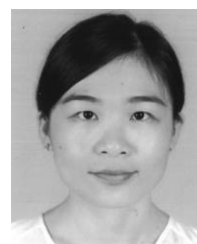
TIE LIU received a Bachelor's degree in Huazhong Agricultural University in 2017. He is studying as a master degree candidate in the School of Electronics and Communication Engineering, Guangzhou University. His research interest is person re-identification.



JIEHAO LIU received a Bachelor's degree in Electronics and Information Engineering from Guangzhou University in 2019. He is currently a master degree candidate in the School of Electronics and Communication Engineering, Guangzhou University. His research interests include face recognition and person re-identification.



LI WANG received a Bachelor's degree in Electronic Engineering from Southeast University, China, in 2009 and received a Ph. D. degree in Physical Electronics from Southeast University, China, in 2015. He is now working in the School of Electronics and Communication Engineering, Guangzhou University. His research interests include brain-computer interfaces, biomedical signal processing, pattern recognition, etc.



SAI ZHAO received the Ph. D degree in communication and information system from Sun Yat-Sen University (SYSU), Guangzhou, China, in 2015, and the Master and Bachelor degrees in Communication Engineering from Central South University, Changsha, China, in 2006 and 2003, respectively. She is currently a lecture in the School of Electronics and Communication Engineering, Guangzhou University. Her current research interests include machine learning in wireless communication, convex optimization, physical layer security and non-orthogonal multiple access.